Landau levels in a band-inverted junction and quantum well

D. Agassi
Naval Surface Warfare Center, White Oak, Maryland 20903-5640
(Received 28 July 1993)

The Landau levels pertaining to a symmetric band-inverted junction and quantum well are calculated in the presence of a magnetic field parallel to the interface. It is shown that the effective band gap is widened at the interfaces, the Landau eigenenergies vary nonmonotonically with distance of the orbit's center from the structure interfaces and that these levels have a noninteger number of harmonic-oscillator energy quanta. The Landau levels in the presence of a magnetic field perpendicular to the interfaces are briefly discussed.

I. INTRODUCTION

There has recently been interest in exploring magnetic-field effects on III-V superlattices when the field is oriented parallel to the interfaces.[1-9] Such a field is referred to hereafter as a parallel field. The motivation for some of these superlattice experiments stems from the premise that the corresponding Landau orbits are oriented normal to the structure interfaces, and consequently, depending on the orbit's center location and radius, electrons are forced to tunnel through one or several interfaces of the structure. The associated cyclotron resonance entails information about physical parameters of this tunneling process, such as the barrier height, effective mass, and epitaxial quality of the structure.[7] This magnetically driven electron motion also leads to new high-field phenomena, such as saturation of the magnetoluminescence maxima energies[1-3] and cyclotron resonance,[4-7] a decrease in magnetoresistance,[9] and a two-peak line shape of the cyclotron resonance.[5] These phenomena reflect the fact that at a high parallel field, the lowest Landau orbits radii are comparable to the superlattice periodicity in the growth direction. As a result, there is competition between superlattice band-structure kinetics and the magnetic motion. This type of competition is absent in Landau levels associated with a magnetic field normal to the interfaces (normal fields). The latter entails orbits entirely contained to a single slab of the layered structure, and therefore pertain to a single band structure.

This work explores parallel field Landau levels in structures unique to narrow-band semiconductors, specifically the symmetric band-inverted junction and quantum well. This choice of structures is motivated by our theme of exposing basic qualitative features. To capture the essence of band inversion, we consider the simplest structures: A bulk band structure of two symmetric, strongly interacting bands, which are band inverted across an interface with no band offset. This bulk band structure and band inversion are realized in the IV-VI semiconductors,[10-13] and bear similarity to the situation in some II-VI and V-V semiconductors, e.g., HgTe vs CdTe (Ref. 10) and Bi vs Bi_xSb_{1-x},[13] respectively. Band-inverted structures are qualitatively different from those studied before[1-9] in two respects: (a) Band symmetry. The Landau levels in the III-V structures are determined by the barrier across the superlattice interface. In contrast, in the symmetric-band-inverted structures there is *no* barrier: The only distinction across the interfaces is the band *symmetry*. (b) Gap states.[11,12] Unlike in III-V superlattices, band-inverted structures support states with energy in the band gap. They decay normal to the interface with a characteristic decay length. These are the gap states. In the presence of a parallel field, electrons tend to revolve normal to the interface in an orbit whose radius is in general larger than the decay length. The competition between the field stretching and the no-field confinement gives rise to a negative-index Landau level.

The analysis of the chosen band-inverted structures exposes the controlling parameters. A case in point is the symmetric junction. We find in particular, that for Landau orbits centered on the interface, there is a substantial net band-gap widening. This result may indicate possibilities of tuning the band gap magnetically. Also, the dispersion relation Eq. (3.4) shows explicitly the two controlling dimensionless parameters: The ratio of the band-gap energy and the cyclotron energy, and the ratio of the orbit's center distance from the interface and the magnetic length.[14] These parameters characterize the physical regimes of the underlying phenomenon, i.e., the interaction of a Landau orbit with an interface. A particularly interesting regime is when both parameters are $\simeq O(1)$. This corresponds to the high-field regime mentioned above,[7] when the band gap and cyclotron resonance energy are comparable, as are the Landau orbit radius and the layered structure length scale.

To evaluate the Landau orbit interaction with two band-inverted interfaces, we consider a quantum well. As is shown below, the second interface reinforces features observed for the junction, in particular the band gap widening at the quantum well center.

The paper is organized as follows: In Sec. II the basic equations and formalism are spelled out. Section III is devoted to the symmetric band-inverted junction and quantum well. Section IV is a discussion and summary. For the sake of self-containment we derive the wave func-

tions for a normal field in the Appendix. These states do not appear in the literature.[12,13] In analogy to similar states in optics, this derivation highlights the evanescent character of gap states.

II. BASIC EQUATIONS

The bulk band structure under consideration is comprised of two symmetric, doubly degenerate, interacting bands at the L point of a cubic lattice. Accounting only for a single isotropic valley, the effective-mass approximation Hamiltonian $\hat{H}_0$ for the envelope function is given by[15]

$$\hat{H}_0(\hat{\mathbf{k}})=\begin{bmatrix} \left[\frac{E_G}{2}+V\right] & -i\hbar c\gamma\hat{\mathbf{k}}\cdot\boldsymbol{\sigma} \\ i\hbar c\gamma\hat{\mathbf{k}}\cdot\boldsymbol{\sigma} & \left[-\frac{E_G}{2}+V\right]I \end{bmatrix}, \tag{2.1}$$

where E_G is the band gap, V is a chosen energy reference point, c is the speed of light, $\boldsymbol{\sigma}=(\sigma_x,\sigma_y,\sigma_z)$ is the Pauli matrices vector, and

$$\hat{\mathbf{k}}=-i\nabla\ ,\quad \gamma=\left[\frac{|E_G|}{2m^*c^2}\right]^{1/2}, \tag{2.2}$$

In (2.2), m^* is the effective mass, and the $\mathbf{k}$ operator pertains to momentum deviation from that of the L point. The effective Hamiltonian (2.1) is identical to the Dirac Hamiltonian,[11] provided that $c^*=\gamma c$ is interpreted as the effective speed of light, and the electron-hole band gap is $E_G=2m^*(c^*)^2$. Unlike the Dirac Hamiltonian, however, the band gap can be negative in an inverted semiconductor.

Note that the band coupling in (2.1) is strong: Typical parameters for IV-VI semiconductors are[10] $\hbar c\gamma\approx 2$ eV Å, $E_G\approx 0.2$ eV, the lattice constant is $a\approx 6$ Å and the momentum deviation from the L point is of the order $k\approx\epsilon\pi/a$, where $\epsilon\ll 1$. These yield for the off-diagonal element of (2.1) $\hbar c\gamma k\approx\epsilon$ eV, which is of the order of the diagonal element $E_G/2\approx 0.1$ eV.

To establish notations, the choice of coordinates, and an equation base line, first consider bulk solutions of (2.1). It can be verified by inspection that the four eigenspinors of (2.1), with eigenenergy E, have the form

$$(\Psi(\mathbf{r}))=e^{i\mathbf{k}\cdot\mathbf{r}}(\chi(\mathbf{k};E))\ . \tag{2.3}$$

In (2.3), $\mathbf{k}=(k_x,k_y,k_z)$ is the momentum, and the spinor $(\chi(\mathbf{k};E))$ satisfies

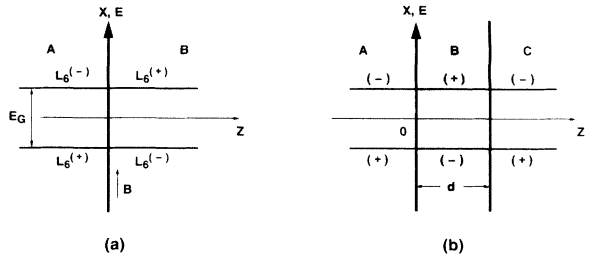

FIG. 1. The band structure and chosen coordinate system for the symmetric junction and quantum well. Interfaces are delineated by bold lines, and the z axis is normal to the interfaces. (a) Indicated are the band symmetries $L_6^{(\pm)}$ for a IV-VI semiconductor band-inverted junction, the energy gap E_G, the magnetic field B chosen parallel to the x direction, and the A and B domains. (b) The quantum-well configuration. The band symmetries are abbreviated by $(\pm)$, the well thickness is d, and the domains are A, B, and C. The magnetic field (not indicated) is as in (a).

$$\hat{H}_0(\hat{\mathbf{k}}\to\mathbf{k})(\chi(\mathbf{k};E))=E(\chi(\mathbf{k};E))\ , \tag{2.4}$$

where the eigenenergy E satisfies the dispersion relation

$$k_t^2+k_z^2=\frac{\lambda(E)\nu(E)}{(\hbar c\gamma)^2}\ ,\qquad \lambda(E)=E-V-\frac{E_G}{2},\quad \nu(E)=E-V+\frac{E_G}{2}\ , \tag{2.5}$$

and the transversal momentum is $\mathbf{k}_t=(k_x,k_y)$. Each of the positive and negative eigenenergies (2.5) are doubly spin degenerate (see the Appendix) and the spectrum is symmetric around $E=V$.

For a layered structure the effective-mass approximation must be supplemented by boundary conditions.[16] Since (2.1) is of first order, the boundary condition across a planar interface at $z=z_I$ [Fig. 1(a)] is[11,12,17]

$$(\Psi(\mathbf{r}))|_{z_I-\epsilon}=(\Psi(\mathbf{r}))|_{z_I+\epsilon}\ , \tag{2.6}$$

where $(\Psi(\mathbf{r}))$ is a four eigenspinor, Eq. (2.3), and $\epsilon\to 0$.

A static magnetic field is incorporated into (2.1) by the standard substitution (in the cgs unit system)

$$\hat{\mathbf{k}}\to\hat{\mathbf{k}}+\frac{|e|}{\hbar c}\mathbf{A}(\mathbf{r})\ ,\quad \mathbf{B}=\nabla\times\mathbf{A}(\mathbf{r})\ . \tag{2.7}$$

In particular, for a parallel field in the x direction [Fig. 1(a)], the electromagnetic vector potential A of (2.7) is chosen as $\mathbf{A}(\mathbf{r})=(0,-B_x z,0)$. A four base eigenspinors of (2.1) are

$$(\Psi_1(\mathbf{r}))=e^{i(k_y y+\chi_\xi\xi)}\begin{bmatrix} \begin{bmatrix}1\\ \varphi\end{bmatrix}D_{p-1}(\xi) \\ \frac{i\hbar c\gamma}{\nu(E)l_H}\left[\begin{bmatrix}1\\ \varphi\end{bmatrix}\varphi\chi_\xi D_{p-1}(\xi)-\begin{bmatrix}1\\ -\varphi\end{bmatrix}i\sqrt{2}D_p(\xi)\right] \end{bmatrix},$$

$$(\Psi_2(\mathbf{r}))=e^{i(k_y y+\chi_\xi \xi)}\begin{bmatrix} \begin{bmatrix}1\\-\varphi\end{bmatrix} D_p(\zeta) \\ \frac{i\hbar c\gamma}{\nu(E)l_H}\left[-\begin{bmatrix}1\\-\varphi\end{bmatrix}\varphi\chi_\xi D_p(\zeta)+\begin{bmatrix}1\\\varphi\end{bmatrix} i\sqrt{2}pD_{p-1}(\zeta)\right]\end{bmatrix},$$

$$\overline{(\Psi_1(\mathbf{r}))}=e^{i(k_y y+\chi_\xi \xi)}\begin{bmatrix} \begin{bmatrix}1\\\varphi\end{bmatrix} D_{p-1}(-\zeta) \\ \frac{i\hbar c\gamma}{\nu(E)l_H}\left[\begin{bmatrix}1\\\varphi\end{bmatrix}\varphi\chi_\xi D_{p-1}(-\zeta)+\begin{bmatrix}1\\-\varphi\end{bmatrix} i\sqrt{2}D_p(-\zeta)\right]\end{bmatrix}, \tag{2.8}$$

$$\overline{(\Psi_2(\mathbf{r}))}=e^{i(k_y y+\chi_\xi \xi)}\begin{bmatrix} \begin{bmatrix}1\\-\varphi\end{bmatrix} D_p(-\zeta) \\ \frac{i\hbar c\gamma}{\nu(E)l_H}\left[-\begin{bmatrix}1\\-\varphi\end{bmatrix}\varphi\chi_\xi D_p(-\zeta)-\begin{bmatrix}1\\\varphi\end{bmatrix} i\sqrt{2}pD_{p-1}(-\zeta)\right]\end{bmatrix},$$

$$\zeta(z)=\frac{\sqrt{2}}{l_H}(z_0-z)\ ,\quad z_0=\varphi k_y l_H^2\ ,$$

and the pertaining dispersion relation for the eigenenergy E is

$$\chi_\xi^2+2p=\left[\frac{l_H}{\hbar c\gamma}\right]^2\lambda(E)\nu(E)\ , \tag{2.9}$$

where p is determined by the boundary conditions (see below). The symbols in (2.8) and (2.9) denote the following: $\varphi=\mathrm{sgn}(B_x)=\pm 1$ indicates the direction of the magnetic field, where $\varphi=1$ corresponds to a field pointing in the positive x-axis direction; $l_H=\sqrt{(\hbar c/|eB_x|)}$ is the magnetic length[14] which is a measure of the lowest Landau orbit extension; $\xi=x/l_H$, $\chi_\xi=l_H k_x$ are the dimensionless x coordinate and momentum; and z_0 is the distance of the Landau orbit center from the interface.

The functions $D_p(\pm\zeta)$ are known as the parabolic cylinder functions.[18–20] They constitute two independent, nonorthogonal solutions of the harmonic-oscillator equation:

$$\left[-\frac{d^2}{d\zeta^2}+\frac{\zeta^2}{4}\right]D_p(\zeta)=(p+\tfrac{1}{2})D_p(\zeta)\ , \tag{2.10}$$

where the p index is in general complex. Since the eigenenergy E is a real number it follows from (2.9) that p in (2.8) must be real. Note that not all eigenspinors (2.8) are mutually orthogonal, though all are independent solutions.

The two solutions $D_p(\pm\zeta)$ obey different boundary conditions at $|\zeta|\to\infty$: $D_p(\zeta)$ converges at $\zeta\to\infty$ and diverges at $\zeta\to-\infty$, except for $p=0,1,2,\ldots$, when it converges at $\zeta\to\pm\infty$

$$\begin{aligned} &D_p(\zeta)\sim e^{-(\zeta^2/2)}\zeta^p \quad \text{for } \zeta\to\infty\ , \\ &D_p(\zeta)\sim e^{-(\zeta^2/2)}\zeta^p+C_p\frac{e^{\zeta^2/2}}{\Gamma(-p)\zeta^{p+1}} \quad \text{for } \zeta\to-\infty\ , \end{aligned} \tag{2.11}$$

where C_p is an uninteresting constant. Similarly, $D_p(-\zeta)$ converges for $\zeta\to-\infty$ and diverges at $\zeta\to\infty$ for $p\neq 0,1,2,\ldots$.[18] When $|p|\gg|\zeta|$ *and* $p<0$ it follows:[18]

$$\begin{aligned} D_p(\pm\zeta)&\simeq\frac{\sqrt{\pi}2^{p/2}}{\Gamma\left[\frac{1-p}{2}\right]}e^{\mp\sqrt{-p-(1/2)}\zeta} \\ &=D_p(0)e^{\mp\sqrt{-p-(1/2)}\zeta}\ . \end{aligned} \tag{2.12}$$

To demonstrate how boundary conditions determine p, consider the bulk solutions (2.8) with boundary conditions of decaying solutions at $\zeta\to\pm\infty$. From (2.11), and the fact that $1/\Gamma(-p)=0$ for $p=0,1,2,\ldots$, it follows that this boundary condition can be satisfied only for $p=n=0,1,2,\ldots$. Hence the textbook one-dimensional harmonic-oscillator solutions, where $D_n(\zeta)$ is related to the Hermite polynomial.[18] In this case, four solutions (2.8) reduce to two spin-degenerate solutions. The exception is when $n=0$ which is nondegenerate since only $(\Psi(\mathbf{r}))_2$ (or its bar counterpart) is a valid solution (also see the Appendix). This exercise implies that whenever the ζ domain is bounded, as in the examples below, the p index is noninteger.[20]

III. BAND-INVERTED JUNCTION AND QUANTUM WELL

To study the interaction of a bulk Landau orbit electron with an interface, we examine two structures, viz., a junction and a quantum well. In keeping with the theme of identifying qualitative features, it is assumed that $E_G(z)$ and $V(z)$ are constant for each domain; hence spinors (2.8) are eigenfunctions in each domain. We also assume for simplicity that $\gamma(z)=\gamma$, which is reasonably satisfied for IV-VI semiconductors.[10]

Since the structures under consideration are translationally invariant in the x and y directions (Fig. 1), the corresponding momenta k_x and k_y, and hence χ_ξ and z_0 of (2.8), are conserved quantities. In contrast, the p index in each domain is in general not a conserved quantity.

A. Band-inverted junction

The simplest configuration involving an interface is a junction, e.g., Fig. 1(a). The corresponding boundary conditions are of decaying solutions on the A side at $\zeta(z)\to+\infty$, and at $\zeta(z)\to-\infty$ on the B side. Accordingly, (2.8) and (2.11) imply the following solutions on each side of the junction:

$$\begin{aligned}(\Psi_A(\mathbf{r}))&=R_A(\Psi_1(\mathbf{r}))+T_A(\Psi_2(\mathbf{r}))\ ,\\ (\Psi_B(\mathbf{r}))&=R_B\overline{(\Psi_1(\mathbf{r}))}+T_B\overline{(\Psi_2(\mathbf{r}))}\ ,\end{aligned}\tag{3.1}$$

where the eigenenergy E and the R and T coefficients are determined from matching the boundary conditions (2.6) at $z_I=0$. Straightforward manipulations yield the dispersion relation, which together with the bulk dispersion relations (2.9) on sides A and B constitute three equations for p_A, p_B, and E for given z_0 and χ_ξ. This dispersion relation is too complex to offer insight, and therefore further simplifying assumptions are introduced. In particular, to isolate effects of band inversion, we consider a symmetric junction depicted in Fig. 1(a), where $|E_G(A)|=|E_G(B)|\equiv E_G$, and $V_A=V_B=0$, and hence (2.9) implies that $p_A=p_B\equiv p$. In the absence of band inversion, i.e., $E_G(A)=E_G(B)$, the junction reduces to a bulk semiconductor which is of no interest. For the nontrivial case of a band-inverted junction, when $E_G(A)=-E_G(B)$, the dispersion relation takes the simple form

$$\Omega D_{p-1}(\zeta_0)D_p(\zeta_0)D_{p-1}(-\zeta_0)D_p(-\zeta_0)+2pW^2(p)=0\ ,\tag{3.2}$$

where

$$\Omega=\left[\frac{l_H E_G}{\hbar c\gamma}\right]^2,\quad \chi_\xi^2+2p=\Omega\left[\left[\frac{E}{E_G}\right]^2-\frac{1}{4}\right],$$

$$\begin{aligned}W^{(+)}_{p-1,p}(\zeta,\zeta)&\equiv W(p)\\ &=D_{p-1}(\zeta)D_p(-\zeta)+D_{p-1}(-\zeta)D_p(\zeta)\\ &=-\frac{1}{p}\frac{\sqrt{2\pi}}{\Gamma(-p)}\ .\end{aligned}\tag{3.3}$$

The symmetric junction dispersion relation (3.2) is a key result of this work. It exposes the two controlling parameters $\zeta_0=\zeta(0)=(\sqrt{2})z_0/l_H$ and Ω. The first determines the degree of the Landau orbit intersection with the interface, and the second is a measure of the strength of the orbit-interface interaction when an intersection takes place. Consider first the latter. Inserting the expressions for the cyclotron frequency of an electron gas,[14] $\omega_c=|eB|/(m^*c)$, the magnetic length l_H and γ [Eq. (2.2)], one obtains $\Omega=2|E_G|/(\hbar\omega_c)$. Thus in the $\Omega\gg1$ regime, electrons are considerably more easily excited between Landau levels than across the band gap. Hence in this regime the junction's Landau levels deviate only slightly from those of the bulk. Large deviations from bulk levels are expected for $\Omega\approx O(1-10)$, when magnetic and electronic transitions compete. This regime corresponds to the strong-field regime.[3,7] The second controlling parameter in (3.2) is ζ_0, i.e., the ratio of the orbit's center distance from the interface, and the lowest Landau orbit extension l_H. Thus $\zeta_0\gg1$ implies that the lowest Landau orbits do not intersect the interface, hence the corresponding levels resemble bulk Landau levels regardless of Ω. Deviations from bulk Landau levels are expected for $\zeta_0\simeq O(1)$, and in particular for $\zeta_0=0$, when the orbits straddle between the two sides of the junction.

Before considering solutions of (3.2), two important limits can be analyzed analytically. First consider orbits centered at the interface, i.e., when $z_0=\zeta_0=0$, and take $\chi_\xi=0$. For $p\geq0$ solutions, both terms in (3.2) are nonnegative; hence to satisfy the dispersion relation both must vanish individually. Noting from (2.12) that $D_p(0)=(\sqrt{(\pi)})2^{p/2}/\Gamma((1-p)/2)$,[18] both terms vanish *only* for $p=1,2,\ldots$, with the conspicuous absence of the $p=0$ Landau level. This is tantamount to a band-gap widening at the interface. The band-gap widening, regardless of the parallel field strength and existence of a barrier is unique to the band-inverted junction. It is interpreted as reflecting the extra energy it takes for a circulating electron to cross into a band-inverted domain. To estimate the effect, assume typical narrow gap semiconductor parameters:[10] $E_G=0.15$ eV, and $\hbar c\gamma\approx2.76$ eV Å (for $m^*/m_0=0.1$). For a field of $B=10$ T, the band-gap widening from Eq. (3.3) is $\Delta E_G=2|E_G|(\sqrt{(\frac{1}{4}+2/\Omega)}-\frac{1}{2})=0.036$ eV, i.e., about 20% of the no-field band gap. For a smaller band gap and effective mass, the relative band-gap widening increases dramatically.

For $p<0$ solutions, the two terms in Eq. (3.2) contribute, resulting in a *single* solution at $p=-\Omega/8$, which, by virtue of (3.3), corresponds to an eigenenergy $E=0$ at the gap center. This is the gap state,[11,12,17] which is an example of a negative-index Landau level. Its physical content becomes clear by considering the no-field (or normal field) configuration in the Appendix: As (A10) shows, the gap state is an evanescent state, of the type encountered in optics. It decays normal to the interface and has no nodes.[19]

It is instructive to examine the decay length for $z_0\simeq0$, when $|p|=\Omega/8\gg|\zeta|$. In this case, Eq. (2.12) yields $D_p(\zeta)\simeq\exp(-z/\lambda_B)$, where the decay length in the presence of the field is $\lambda_B^{-1}=[\sqrt{(-1+\Omega/4)}]/l_H$. Comparing this to the no-field decay length [Eq. (A13)] $\lambda_0^{-1}=E_G/(2\hbar c\gamma)=\sqrt{(\Omega)}/(2l_H)$, we see explicitly the parallel field-stretching effect, mentioned in Sec. I, in that $\lambda_B^{-1}<\lambda_0^{-1}$. The above estimate indicates that for $\Omega\leq O(10)$ this effect is appreciable. The numerical results below corroborate the stretching effect for the other z_0 values. Note that the parallel field effect on gap states is opposite to its confinement effect on conduction and valence no-field states.

The other analytic limit of (3.2) is that of Landau orbits centered far from the interface, i.e., when $|\zeta_0|\to\infty$.

These orbits do not intersect the interface, and hence are expected to resemble bulk Landau levels. Indeed, employing the asymptotic expansion (2.11), it follows that

$$\lim_{\zeta\to\infty} D_p(\zeta)D_p(-\zeta)\approx\frac{C_1}{\zeta\Gamma(-p)}+C_2\zeta^{2p}e^{-\zeta^2/2}\ . \tag{3.4}$$

Consequently, for $|\zeta|\gg 1$ the first term in (3.4) dominates, and only p values near nonzero integers are solutions for (3.2).

Having analyzed (3.2) in two limits, it is instructive to solve it numerically for $p(z_0)$. We consider a case when $E_G=0.1$ eV, and $B=6$ T, which yields $l_H=257/(\sqrt{(B[\mathrm{T}]}))$ Å $\simeq 105$ Å, and $\Omega=14.56$. As discussed above, this Ω value is sufficiently small to expose competition between electronic and magnetic transitions, and l_H is not too large to render numerical calculations excessive. The results are given in Fig. 2. Since all Landau energies emanate from the same Hamiltonian, the ensuing eigenenergies do not cross, barring incidents of accidental degeneracy.

To discuss Fig. 2 consider first $z_0=-300$ Å, which is characterized by $|z_0|\gg l_H$. Since in this case the lowest orbits do not intersect the interface, we expect to recover the lowest bulk Landau levels. Indeed, the $p\simeq 0$ level is slightly negative *and* nondegenerate, the $p\simeq 1$ levels constitute a slightly split doublet, the $p\simeq 2$ doublet splitting is larger yet, and the next-higher Landau level cannot be identified unambiguously. The doublet splitting represents the lifting of the bulk Landau-level degeneracy by the orbit interaction with the interface. To corroborate this interpretation, note that the estimated orbit radius is[14] $r_p=1.414(p+0.5)l_H$. For the $p=0$ and 1 levels, the radii are 74 and 222 Å, respectively, considerably smaller than z_0; hence the small shift and splitting. The $p\simeq 2$ Landau orbit, on the other hand, has an estimated radius of $r_p\simeq 371$ Å $>z_0$, resulting in an interface intersection and a large doublet splitting.

As z_0 decreases, interface-orbit interaction sets in. We discuss separately the $p\geq 0$ and $p<0$ levels. The latter gap state is monotonically decreasing toward the value $p=-\Omega/8=-1.82$ at the interface. The sharp drop at a distance $|z_0|\simeq 200$ Å (Fig. 2) signals the onset of orbit-interface interaction for the gap state. The fact that this interaction starts at z_0 considerably larger than the no-field decay length $(k_z)^{-1}=(2\hbar c\gamma)/E_G\simeq 55$ Å (A13) reflects the stretching effect of the parallel field, discussed in Sec. I. The $p\geq 0$ Landau levels vary with z_0 quite differently. Note first that the splitting of the doubly degenerate levels increases with decreasing z_0, with one level moving down in energy and the other slightly up. This trend cannot continue with decreasing z_0 since different levels repel each other. As a result the Landau energies vary with z_0 nonmonotonically, going up and down, thereby giving rise to minima and maxima at different distances from the interface. This pattern implies magnetically induced carrier redistribution with regard to distance from the interface.[9] This phenomenon is likely to be reflected in observables such as magnetoresistance.

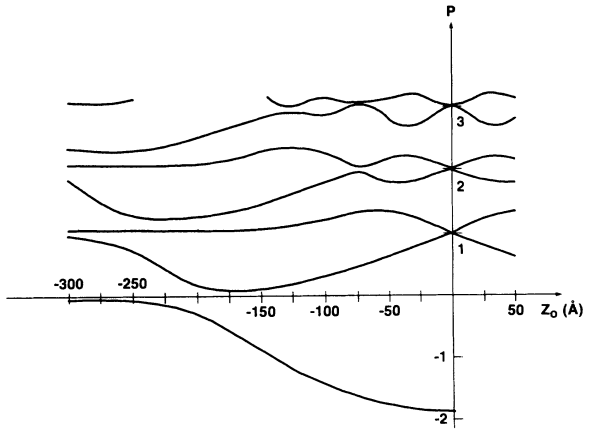

FIG. 2. The calculated lowest $p(z_0)$ curves for a symmetric band inverted junction, Eq. (3.2). The parameters are $\Omega=14.56$, and $l_H\simeq 105$ Å, corresponding to $E_G=0.1$ eV, $m^*/m_0=0.1$, and $B=6$ T. The plots, symmetric about $z_0=0$, are displayed primarily for the range $z_0\leq 0$ Å. The corresponding eigenenergy is given by (3.3).

The accidental degeneracies at $z_0=0$ of the $p=1,2,\ldots$ levels are unique to the symmetric junction.

For a nonsymmetric junction, a similar level structure is expected, though one which is more complex. A case in point is the symmetrically aligned junction where $V_A=V_B=0$[13]. Subtracting the dispersion relations (2.9) on both sides of the junction gives

$$p_B-p_A=\left[\frac{l_H}{2\hbar c\gamma}\right]^2[E_G^2(A)-E_G^2(B)]\ . \tag{3.5}$$

Relation (3.5) implies Landau levels where the p index has opposite signs on both sides of the junction, in addition to levels for which the p indices have the same sign on both sides of the junction. The latter are already present in the symmetric junction. The former arise when the Landau-level energy at the interface is smaller than the band offset. These Landau levels are interpreted as skipping states,[5,21] with a cycloidlike trajectory on one side of the junction, and a Gaussian decay on the other side.

B. An inverted quantum well

The motivation for considering a quantum well is to find out how effects encountered for a junction, such as the effective band-gap widening at the interface, are modified when the Landau orbit interacts with *two* interfaces. Results for the quantum well, combined with those for the junction, yield insight into the more complex case of a superlattice.

In the vein of focusing on key qualitative features, we consider a symmetric inverted quantum well, Fig. 1(b), where $E_G(A)=-E_G(B)=E_G(C)\equiv E_G$, and $V_A=V_B=V_C=0$, and therefore the p index is conserved. Tedious algebra yields the dispersion relation

$$\Omega^2 W^{(-)}_{p,p}(\zeta_0,d)W^{(-)}_{p-1,p-1}(\zeta_0,d)D_p(-\zeta_d)D_{p-1}(-\zeta_d)D_p(\zeta_0)D_{p-1}(\zeta_0)$$
$$+2p\Omega W^2(p)[-2D_p(-\zeta_d)D_{p-1}(-\zeta_d)D_p(\zeta_0)D_{p-1}(\zeta_0)$$
$$+D_p(-\zeta_0)D_{p-1}(-\zeta_0)D_p(\zeta_0)D_{p-1}(\zeta_0)+D_p(-\zeta_d)D_{p-1}(-\zeta_d)D_p(\zeta_d)D_{p-1}(\zeta_d)]+(2pW^2(p))^2=0\ , \tag{3.6}$$

where the anti-Wronskian [compare with (3.3)] is defined as

$$W^{(-)}_{p,p}(\zeta_0,\zeta_d)\equiv D_p(\zeta_0)D_p(-\zeta_d)-D_p(-\zeta_0)D_p(\zeta_d)\ . \tag{3.7}$$

The symbols in (3.6) signify the following: Ω and $W(p)$ are defined in (3.3) and $\zeta_d\equiv\zeta(z=d)=((\sqrt{2})/l_H)(z_0-d)$. Note that the thickness enters only via the variable ζ_d, which involves the distance of the second interface from the Landau orbit center z_0. The dispersion relation (3.6) is solved for p, and the ensuing eigenenergy is obtained from the dispersion relation (3.3).

Before discussing numerical solutions of (3.6), we check two analytic limits where physical arguments imply the expected result. The first is the limit of an infinitely thick quantum well, namely $d\to\infty$ and finite z_0. In this limit we expect to recover the symmetric junction dispersion relation (3.2), since $d\to\infty$ implies that Landau orbits can intersect only the $z=0$ interface. Inserting the asymptotic expression (2.11) for the ζ_d-dependent terms in (3.6) yields that the leading terms are the second term in the square brackets, and the last term in (3.6). Their sum is exactly the left-hand side of (3.2), multiplied by a factor, diverging as $\zeta_d\to\infty$; hence the dispersion relation (3.2) is recovered.

A second analytic check of (3.6) pertains to the gap states. Their no-field dispersion relation is known[17] and should be obtainable from (3.6) in the weak-field limit. In the $B\to 0$ limit, it follows from (3.3) that $\Delta=(\sqrt{2})d/l_H\to 0$, $\Omega\to\infty$, and $|p|\simeq O(\Omega)$ and is negative. Consequently the asymptotic approximation (2.12) applies. Inserting it in *all* terms of (3.6) yields

$$4p(1+\coth[\Delta\sqrt{-p}\ ])+\Omega=0\ . \tag{3.8}$$

This is the correct dispersion relation[17] with the substitutions $2p\to l_H^2k_z^2$ from (2.9), and $k_z\equiv iK_z$ for a decaying gap state. Note that the $d\to\infty$ limit of (3.8) yields the value $p=-\Omega/8$, which transcribes to a decay length $|k_z^{-1}|=2\hbar c\gamma/E_G$. This is the correct result since, in the regime where d exceeds the gap states decay length, the two interfaces do not interact and hence the one-interface (junction) result is expected.

Figures 3 and 4 depict the calculated $p(z_0)$ curves from (3.6) for a quantum well with the same parameters as the junction in Fig. 2. In Fig. 3, z_0 is varied, while the well thickness is fixed at $d\simeq l_H$. Consider first the Landau levels inside the well. Note the two gaps states and an enhancement of the band-gap widening in comparison to that in Fig. 2, in particular at the well center. This enhancement is interpreted as resulting from the extra energy it takes for an electron to traverse two band-inverted interfaces. Another feature is that the accidental level degeneracy at $z_0=0$ encountered for the junction (Fig. 2) is broken in the presence of the second interface. Outside the quantum well, the Landau levels behave much like those of the junction (Fig. 2), except that local minima positions are shifted and accentuated. This corroborates the comment above that a parallel field induces considerable carrier redistribution.

To elaborate on the thickness dependence, in Fig. 4 we calculate the Landau levels for two z_0 values and a variable thickness. Consider first Fig. 4(a), depicting the case of orbits whose centers are located at the left interface of the quantum well. When $d\gg l_H$, e.g., at $d=300$ Å, the levels pattern is that of a junction: A gap state, the missing $p=0$ state, and higher doubly degenerate levels. As d decreases, at about $d\simeq 2l_H$ ($d\simeq 200$ Å) the lowest orbit begins to intersect the second interface, resulting in two gap states. As d keeps decreasing, at the extreme of $d\ll l_H$, electrons in Landau orbits spend most of their time in the same band-structure environment, and hence bulk Landau levels emerge. This trend is manifested in the upturn of the gap states at small d. In Fig. 4(b) the lowest Landau levels at the well's center are calculated. The interesting feature is the band-widening maximum at $d\simeq 150$ Å, where $l_H=105$ Å. This value represents a situation where the lowest $p>0$ orbit is spread between the inside and outside of the quantum well.

IV. DISCUSSION

As has been shown above, two important manifestations of band inversion are the band-gap widening at the interface, or equivalently, the absence of the $p=0$ Landau level, and the gap states in the band gap. The band-

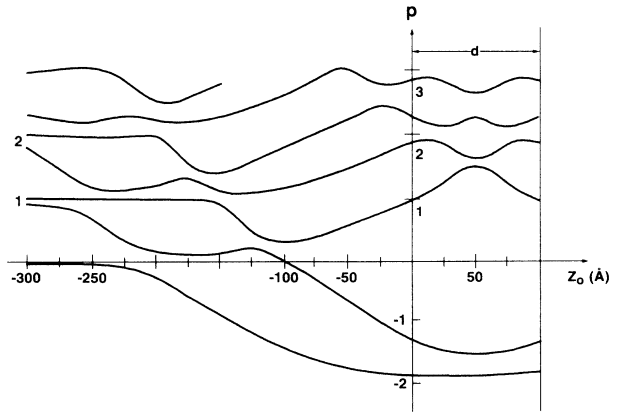

FIG. 3. The calculated lowest $p(z_0)$ curves for a symmetric quantum well, Eq. (3.6). The parameters are as in Fig. 2, and the thickness is $d=100$ Å$\simeq l_H$. The plots, symmetric about $z_0=d/2$, are displayed for the range $z_0\le d$.

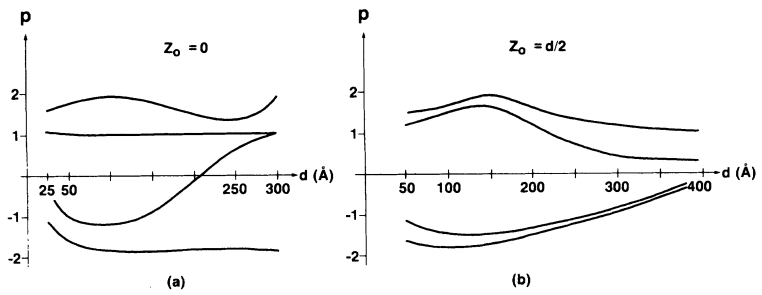

FIG. 4. Same as Fig. 3, except that z_0 is fixed at the values $z_0=0$ and $d/2$ and the well thickness is varied.

gap widening effect is substantial: For typical parameters of narrow-band semiconductors[10] ($E_G=0.15$ eV and $m^*/m_0=0.1$), a field of 10 T induces a relative band-gap widening of the magnitude $\Delta E_G/|E_G|\simeq 4/\Omega\simeq 0.2$ and is linear in the applied field [see Eq. (3.3)]. This amount of band-gap widening is comparable to that observed in diluted magnetic semiconductors (DMS) such as $Hg_{1-x}Mn_xTe$.[22] The underlying mechanisms, however, are quite different: In a band-inverted structure the band-gap widening is an interface phenomenon, due to a specific symmetry variation of the band structure, whereas in DMS band-gap widening is a bulk phenomenon resulting from a magnetic exchange interaction between magnetic impurities and conduction carriers. We expect that one manifestation of this difference is the temperature dependence of the band-gap widening. In inverted structures, the band gap is expected to increase with temperature, provided Ω is kept fixed, following the increase of E_G.[10] In DMS, the temperature effect is to reduce and saturate the band-gap widening.[23]

Another consequence of band inversion is the formation of Landau-level energy minima at a distance from an interface. A case in point is the lowest $p>0$ Landau level in Fig. 2. Note that in the absence of band inversion such minima are considerably shallower.[2,6,7] There, the $p=0$ Landau level at large z_0 maintains its p value at $z_0\simeq 0$, and hence for intermediate z_0, the z_0 variation is expected to be shallow.

The Landau levels for a parallel field studied here differ in several important respects from those associated with a field normal to the interfaces, which are derived in the Appendix. The basic difference stems from the different types of motion in both cases: For a normal field, electrons do not traverse through an interface, whereas for a parallel field they traverse several band-structure environments in the course of a revolution. One manifestation of this difference is that for a normal field the Landau eigenenergies are constants, whereas for a parallel field they depend on the orbit distance from interfaces in the structure. Another manifestation pertains to the gap states. For a normal field the gap states obey the dispersion relation [Eqs. (A11) and (A13)] $E_{\rm gap}=\pm\hbar c\gamma|k_t|$, where $\mathbf{k}_t=(k_x,k_y)$, and decay exponentially away from the interface with a decay length $|k_z|^{-1}=2\hbar c\gamma/E_G$. For a parallel field, gap states do not obey a linear dispersion relation, e.g., Fig. 2, and the wave function decays as a Gaussian with a decay length larger (stretched) than the no-field value.

The validity of the underlying effective-mass approximation (EMA) may be questionable for strong fields, i.e., when $l_H\ll d$, when the granularity of the structure is probed.[1,7] While it is difficult to assess the degree of the EMA failure, note that our analysis and examples, e.g., Fig. 3, pertain to modest excursions out of the regimes of validity.

The present system bears some similarity to recent experiments on magnetotunneling of electrons through the interface of He_4 and air, in the presence of a parallel field.[24] In particular, the observed strong-field dependence of the tunneling probability may have an analog in the structures considered here. For the example of a quantum well (Fig. 3), the Landau-level z_0 variation forms a magnetically controlled barrier. As the field varies so does the barrier height, and hence also the Fermi-level position with respect to the barrier height. As a result, the exponential dependence of the tunneling probability on the barrier–Fermi-level energy distance implies a strong dependence of the former on the parallel field.

In summary, the Landau levels for a symmetric junction and quantum well have been calculated. This type of Landau level has a noninteger number of energy quanta. The analytic formulation of these systems exposes the controlling physical parameters: The ratio of the gap energy and cyclotron frequency, and the ratio of the magnetic length and the other length scales in the system. Band inversion gives rise to unique features, such as band-gap widening at the interface, pronounced minima in the Landau-level energies as a function of the distance from interfaces, and negative index Landau levels associated with gap states.

ACKNOWLEDGMENTS

Our thanks to Dr. J. R. Cullen and Dr. R. S. Allgaier for many insightful discussions. This work was sponsored by the Independent Research fund of NSWC.

APPENDIX

In this appendix we derive the eigenfunctions for an abrupt junction in the presence or absence of a magnetic field perpendicular to the interface. The principal purpose of the present derivation is to demonstrate the evanescent character of the gap states,[11,12] and thereby clarify their physical content. The derivation complements existing discussions of the gap states by explicitly constructing the band states.

For a magnetic field $\mathbf{B}=(0,0,B_z)$ (Fig. 1) and elec-

tromagnetic vector potential $\mathbf{A}(\mathbf{r})=(0,xB_z,0)$ in (2.7), the bulk four eigenfunctions are

$$(\chi(\xi))=e^{i(k_y y+\chi_\zeta \zeta)}\begin{bmatrix} c_1(U)\psi_{n-1}(\xi)+c_2(V)\psi_n(\xi) \\ c_3(U)\psi_{n-1}(\xi)+c_4(V)\psi_n(\xi)\end{bmatrix},$$
$$(U)=\frac{1}{2}\begin{bmatrix}1+\varphi\\1-\varphi\end{bmatrix},\quad (V)=\frac{1}{2}\begin{bmatrix}1-\varphi\\1+\varphi\end{bmatrix}, \tag{A1}$$
$$\xi=(x_0+x)/l_H\ ,\quad x_0=\varphi k_y l_H^2\ ,$$

where $\varphi=\mathrm{sgn}(B_z)=\pm 1$ is the orientation of the magnetic field ($\varphi=1$ corresponds to a field pointing along the positive z axis), $\chi_\zeta=l_H k_z$ [$\mathrm{Re}(\chi_\zeta)\geq 0$] and $\zeta=z/l_H$ are the dimensionless z momentum and coordinates, and $-x_0$ is the center of the Landau orbit. The harmonic-oscillator functions $\psi_n(\xi)$ satisfy the canonical equation[20]

$$\left[-\frac{d^2}{d\xi^2}+\xi^2\right]\psi_n(\xi)=(2n+1)\psi_n(\xi)\ ,\quad n=0,1,2,\ldots, \tag{A2}$$

and the corresponding bulk dispersion relation is

$$\chi_\zeta^2+2n=\left[\frac{l_H}{\hbar c\gamma}\right]^2\lambda(E)\nu(E)\ ,\quad n=0,1,2,3,\ldots\ . \tag{A3}$$

The non-negative integer n values in (A3) are dictated by the boundary condition of decaying solutions at $\xi\to\pm\infty$ (see Fig. 1).

The spinor coefficients in (A1) satisfy the matrix equation

$$\begin{bmatrix}-\lambda(E)I & -i\hbar c\gamma\mathbf{k}_n\cdot\boldsymbol{\sigma}\\ i\hbar c\gamma\mathbf{k}_n\cdot\boldsymbol{\sigma} & -\nu(E)I\end{bmatrix}\begin{bmatrix}c_1\\c_2\\c_3\\c_4\end{bmatrix}=0\ , \tag{A4}$$
$$\mathbf{k}_n=(0,\sqrt{2n}\ ,\varphi\chi_\zeta)\ ,$$

which has the following symmetry:[12]

$$[\hat{H}_0,\hat{T}]=0\ ,\quad \hat{T}=\begin{bmatrix}\hat{\sigma}_x & 0\\ 0 & -\hat{\sigma}_x\end{bmatrix},\quad \hat{T}^2=I\ , \tag{A5}$$

and H_0 is the matrix in (A4). Consequently, the (c) eigenspinors are eigenvectors of (A4) and the T operator in (A5). This leads to the form

$$\begin{bmatrix}c_1\\c_2\\c_3\\c_4\end{bmatrix}\equiv(c)(\tau,\mathbf{k}_n)=\begin{bmatrix}\begin{bmatrix}1\\\tau\end{bmatrix}\\ \dfrac{i\hbar c\gamma}{\nu(E)}(\mathbf{k}_n\cdot\boldsymbol{\sigma})\begin{bmatrix}1\\\tau\end{bmatrix}\end{bmatrix},$$
$$\tau=\pm 1\ ,\quad n=1,2,3,\ldots\ . \tag{A6}$$

Note that (A6) implies that the $n\neq 0$ eigenspinors are doubly τ degenerate, in addition to their $\pm\chi_\zeta$ degeneracy [see (A3)], while the $n=0$ eigenspinor is not τ degenerate.

The effect of an interface at $z=z_I$ on the bulk states (A6) is to lift the $\pm\chi_\zeta$ degeneracy, since an interface breaks the translational invariance in the z direction. The τ degeneracy and the n quantum number, on the other hand, are conserved by the boundary conditions (2.6). Consequently, the conduction- and valence-band states can be readily constructed as combinations of reflected and transmitted waves, sharing the same $|\chi_\zeta|$. With $|R_{A,B}|\geq 1$, and transmission coefficients satisfying $T_{A,B}=1+R_{A,B}$, we choose for the band states

$$\begin{aligned}(\Psi_{\vec{A}})&=e^{ik_y y}[R_A e^{i\chi_\zeta(A)\zeta}(\alpha)+e^{-i\chi_\zeta(A)}(\bar{\alpha})]\ ,\\ (\Psi_{\vec{B}})&=e^{ik_y y}[T_B e^{i\chi_\zeta(B)\zeta}(\beta)]\ ,\\ (\Psi_{\overleftarrow{A}})&=e^{ik_y y}[T_A e^{-i\chi_\zeta(A)\zeta}(\bar{\alpha})\ ,\\ (\Psi_{\overleftarrow{B}})&=e^{ik_y y}[R_B e^{-i\chi_\zeta(B)\zeta}(\bar{\beta})+e^{i\chi_\zeta(B)}(\beta)]\ ,\end{aligned} \tag{A7}$$

where the basis spinors in (A7), e.g., $(\alpha),(\bar{\alpha})$, correspond to A-side spinors of the form (A1), with c eigenspinors of the form (A4) and

$$\begin{aligned}&(c)_{(\alpha)}=(c)(\tau,\mathbf{k}_n(A))\ ,\quad (c)_{(\bar{\alpha})}=(c)(\tau,\overline{\mathbf{k}_n(A)})\ ,\\ &\mathbf{k}_n(A)=\frac{1}{l_H}(0,\sqrt{2n},\ \varphi\chi_\zeta(A))\ ,\\ &\overline{\mathbf{k}_n(A)}=\frac{1}{l_H}(0,\sqrt{2n}\ ,-\varphi\chi_\zeta(A))\ ,\end{aligned} \tag{A8}$$

The R and T coefficients are determined by matching the boundary condition (2.6) across the interface. This gives, e.g., for the A-side the equations

$$\begin{aligned}&R_A^2 a_2+R_A a_1+a_0=0\ ,\\ &a_2=q_A^2[\mathbf{k}_n(A)\cdot\mathbf{k}_n(A)]+q_B^2[\mathbf{k}_n(B)\cdot\mathbf{k}_n(B)]\\ &\qquad -2q_A q_B[\mathbf{k}_n(A)\cdot\mathbf{k}_n(B)]\ ,\\ &a_1=2\{q_A^2[\mathbf{k}_n(A)\cdot\overline{\mathbf{k}_n}(A)]+q_B^2[\mathbf{k}_n(B)\cdot\mathbf{k}_n(B)]\\ &\qquad -2q_A q_B(k_n)_t^2\}\ ,\\ &a_0=q_A^2[\overline{\mathbf{k}_n}(A)\cdot\overline{\mathbf{k}_n}(A)]+q_B^2[\mathbf{k}_n(B)\cdot\mathbf{k}_n(B)]\\ &\qquad -2q_A q_B[\overline{\mathbf{k}_n}(A)\cdot\mathbf{k}_n(B)]\ ,\\ &T_B=1+R_A,\quad q_A=\frac{\hbar c\gamma_A}{\nu_A(E)},\quad q_B=\frac{\hbar c\gamma_B}{\nu_B(E)}\ .\end{aligned} \tag{A9}$$

In this scheme, where conduction- and valence-band states are combinations of interface-reflected and interface-transmitted waves, evanescent waves are solutions without an incoming-wave source term, i.e., from (A7)

$$R_A=R_B=0\ . \tag{A10}$$

Condition (A10) implies that $a_0=0$ [Eq. (A9)], which yields the dispersion relation

$$2\hbar c|(k_t)_n|=\left[-\frac{(\lambda_A\nu_B-\lambda_B\nu_A)^2}{(\lambda_A\gamma_B-\lambda_B\gamma_A)(\nu_A\gamma_B-\nu_B\gamma_A)}\right]^{1/2}, \tag{A11}$$

where $\lambda_{A,B}$ and $\nu_{A,B}$ are the A side and B-side constants defined in (2.5). This dispersion relation is precisely the

dispersion relation for the gap states,[11,12] generalized for an arbitrary junction.

The above discussion is readily transcribed to the limit of no magnetic field. The bulk solutions in this case are of the form

$$(\chi(\xi))=e^{i(k_x x+k_y y+\chi_\xi \xi)}\begin{bmatrix} c_1 \\ c_2 \\ c_3 \\ c_4 \end{bmatrix}, \tag{A12}$$

where the c eigenspinors in (A12) are given by (A6), and (A7)–(A11) remain valid with the substitution $(\mathbf{k}_n)_t=(0,\sqrt{2n}\,)/\ell_H \rightarrow \mathbf{k}_t=(k_x,k_y)$. In particular, the gap states dispersion relation (A11) can be expressed in the equivalent form[17]

$$[k_z(A)+k_z(B)]^2=\frac{(\lambda_A\gamma_B-\lambda_B\gamma_A)(\nu_A\gamma_B-\nu_B\gamma_A)}{[\hbar c\gamma_A\gamma_B]^2}. \tag{A13}$$

[1] J. C. Maan, in *Two Dimensional Systems, Heterostructures and Superlattices,* edited by G. Bauer, F. Kuchar, and H. Heinrich, Springer Series in Solid State Sciences Vol. 53 (Springer, Berlin, 1984), p. 183.

[2] G. Belle, J. C. Maan, and G. Weimann, Solid State Commun. **56**, 65 (1985).

[3] G. Belle, J. C. Maan, and G. Weimann, Surf. Sci. **170**, 611 (1986).

[4] T. Duffield, R. Bhat, M. Koza, F. DeRosa, D. M. Hwang, P. Grabbe, and S. J. Allen, Jr., Phys. Rev. Lett. **56**, 2724 (1986).

[5] T. Duffield, R. Bhat, M. Koza, F. DeRosa, K. M. Rush, and S. J. Allen, Jr., Phys. Rev. Lett. **59**, 2693 (1987).

[6] T. Duffield, R. Bhat, M. Koza, D. M. Hwang, F. Derosa, P. Grabbe, and S. J. Allen, Jr., Solid State Commun. **65**, 1483 (1988).

[7] S. J. Allen *et al.,* in *Electronic Properties of Multilayers and Low Dimensional Semiconductors Structures,* edited by Chamberlain, L. Eaves, and J. C. Portal (Plenum, New York, 1990), p. 117.

[8] M. M. Dignam and J. E. Sipe, Phys. Rev. B **45**, 6819 (1992).

[9] R. J. Nicholas, in *Physics and Applications of Quantum Wells and Superlattices,* edited by E. E. Mendez and K. von Klitzing (Pergamon, London, 1987), p. 217.

[10] G. Nimtz and B. Schlicht, in *Narrow-Gap Semiconductors,* Springer Tracts in Modern Physics (Springer-Verlag, Berlin, 1985), pp. 1–119.

[11] O. A. Pankratov and B. A. Volkov, in *Landau Level Spectroscopy,* edited by G. Landwehr and E. I. Rashba (North-Holland, Amsterdam, 1991), pp. 817–854.

[12] D. Agassi and V. Korenman, Phys. Rev. B **37**, 10 095 (1988).

[13] D. Agassi and T. K. Chu, Appl. Phys. Lett. **51**, 2227 (1987).

[14] C. Kittel, *Introduction to Solid State Physics,* 4th ed. (Wiley, New York, 1971), pp. 342–350; J. Callaway, *Quantum Theory of the Solid State* (Academic, New York, 1974), Vol. B, p. 491.

[15] P. A. Wolf, J. Phys. Chem. Solids **25**, 1057 (1964).

[16] G. Bastard, *Wave Mechanics Applied to Semiconductor Heterostructures* (Halsted, New York, 1988).

[17] V. Korenman and H. D. Drew, Phys. Rev. B **35**, 6446 (1987).

[18] I. S. Gradshteyn and I. M. Ryzhik, *Tables of Integrals and Products* (Academic, New York, 1965), p. 1064; J. C. P. Miller in *Handbook of Mathematical Functions,* edited by M. Abramowitz and I. A. Stegun (National Bureau of Standards, Washington, DC, 1964), p. 689.

[19] Higher Transcendental Functions, edited by A. Erdelyi (McGraw-Hill, New York, 1953), Vol. II, Chap. VIII.

[20] E. Merzbacher, *Quantum Mechanics* (Wiley, New York, 1970), pp. 70–79.

[21] R. S. Allgaier, Phys. Rev. B **8**, 4470 (1973); J. F. Koch and J. D. Jensen, Phys. Rev. **184**, 643 (1969).

[22] C. Rigaux, in *Semiconductors and Semimentals,* edited by J. K. Furdyna and J. Kossut (Academic, Boston, 1988), Vol. 25, p. 242.

[23] H. Pascher, E. J. Fanter, G. Bauer, W. Zawadzki, and M. V. Ortenberg, Solid State Commun. **48**, 461 (1983).

[24] L. Menna, S. Yucel, and E. Y. Andrei, Phys. Rev. Lett. **70**, 2154 (1993).